

# SCIENTIFIC REPORTS

OPEN

## N<sub>2</sub>O formation by nitrite-induced (chemo)denitrification in coastal marine sediment

Julia M. Otte<sup>1,2</sup>, Nia Blackwell<sup>1,2</sup>, Reiner Ruser<sup>3</sup>, Andreas Kappler<sup>1,4</sup>, Sara Kleindienst<sup>1,2</sup> & Caroline Schmidt<sup>1</sup>

Nitrous oxide (N<sub>2</sub>O) is a potent greenhouse gas that also contributes to stratospheric ozone depletion. Besides microbial denitrification, abiotic nitrite reduction by Fe(II) (chemodenitrification) has the potential to be an important source of N<sub>2</sub>O. Here, using microcosms, we quantified N<sub>2</sub>O formation in coastal marine sediments under typical summer temperatures. Comparison between gamma-radiated and microbially-active microcosm experiments revealed that at least 15–25% of total N<sub>2</sub>O formation was caused by chemodenitrification, whereas 75–85% of total N<sub>2</sub>O was potentially produced by microbial N-transformation processes. An increase in (chemo)denitrification-based N<sub>2</sub>O formation and associated Fe(II) oxidation caused an upregulation of N<sub>2</sub>O reductase (typical *nosZ*) genes and a distinct community shift to potential Fe(III)-reducers (*Arcobacter*), Fe(II)-oxidizers (*Sulfurimonas*), and nitrate/nitrite-reducing microorganisms (*Marinobacter*). Our study suggests that chemodenitrification contributes substantially to N<sub>2</sub>O formation from marine sediments and significantly influences the N- and Fe-cycling microbial community.

Nitrous oxide (N<sub>2</sub>O) is one of the most important long-lived greenhouse gases with an atmospheric lifetime of 131 ± 10 years<sup>1</sup>. N<sub>2</sub>O has a 265 or 298 (without or with climate-carbon feedbacks, respectively)<sup>2</sup> times higher global warming potential than the same mass of CO<sub>2</sub> and contributes up to 6% to the overall global radiative forcing<sup>3</sup> by participating in the depletion of the stratospheric ozone layer through photochemical nitric oxide (NO) production<sup>4</sup>. Globally, annual N<sub>2</sub>O emissions are derived from soils (6.6 Tg per year), wetlands (0.17 Tg per year), rice paddies (2.8 Tg per year), wildfires and biomass burning (0.1 Tg per year), rivers (<0.6 Tg per year), lakes (<0.04 Tg per year), open oceans (3.8 Tg per year), as well as in coastal marine sediments (1.7 Tg per year)<sup>5</sup>. A variety of biotic and abiotic processes generate N<sub>2</sub>O but the specific contribution of the individual processes to the global N<sub>2</sub>O budget is still uncertain<sup>6</sup>. Processes forming N<sub>2</sub>O include: (1) nitrification (oxidation of ammonia to nitrate)<sup>7</sup>, (2) denitrification (reduction of nitrate to NO, N<sub>2</sub>O or N<sub>2</sub>)<sup>8</sup> by fungi, archaea, and bacteria, (3) dissimilatory nitrate reduction to ammonium (DNRA)<sup>9</sup>, (4) nitrifier-denitrification (ammonia oxidation to nitrite followed by the reduction of nitrite to nitric oxide)<sup>10,11</sup> and (5) nitrite-induced (chemo)denitrification, e.g. by ferrous iron (Fe(II))<sup>12,13</sup>. Nitrous oxide is also produced by anaerobic methane-oxidizing bacteria<sup>14</sup>, ammonia-oxidizing archaea<sup>15</sup>, and anammox bacteria<sup>16</sup>. It has been suggested that microbial N<sub>2</sub>O production is dominated by nitrification and denitrification<sup>17</sup>.

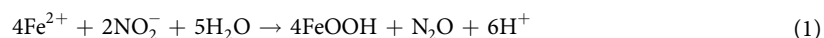
Microbial denitrification proceeds via several metabolic steps, which can be followed by the activity of the respective enzymes. The only known microbially mediated reduction of N<sub>2</sub>O is the microbial reduction to N<sub>2</sub> via (a) typical *nosZ*-encoded N<sub>2</sub>O reductases<sup>18,19</sup>. Nitrate reduction can be mediated by microorganisms that couple Fe(II) oxidation to nitrate reduction (NRFeOx)<sup>20</sup>. Several cultures of NRFeOx have been isolated from various environments and have been shown to be involved in the emission of high levels of N<sub>2</sub>O<sup>21</sup>. Only recently it has been proven that the oxidation of Fe(II) during NRFeOx is an abiotic process stimulated by nitrite and Fe(II)<sup>22</sup>. This abiotic process is triggered by the biotic production of reactive nitrogen species during denitrification<sup>22</sup>. The rapid abiotic reduction of nitrite by Fe(II) is an important N<sub>2</sub>O source in nature and termed chemodenitrification<sup>23,24</sup>.

<sup>1</sup>Geomicrobiology, Center for Applied Geosciences, University of Tübingen, Tübingen, Germany. <sup>2</sup>Microbial Ecology, Center for Applied Geosciences, University of Tübingen, Tübingen, Germany. <sup>3</sup>Fertilization and Soil Matter Dynamics, Institute of Crop Science, University of Hohenheim, Stuttgart, Germany. <sup>4</sup>Center for Geomicrobiology, Aarhus University, Aarhus, Denmark. Correspondence and requests for materials should be addressed to A.K. (email: [andreas.kappler@uni-tuebingen.de](mailto:andreas.kappler@uni-tuebingen.de))

Received: 11 November 2018

Accepted: 12 July 2019

Published online: 31 July 2019



Chemodenitrification could be driven by the presence of Fe(II) that is produced by heterotrophic Fe(III)-reducing microorganisms<sup>23</sup>, as well as by the availability of nitrite, that is produced during the reduction of nitrate by heterotrophic denitrifying bacteria<sup>18</sup>. The abiotic production of N<sub>2</sub>O via chemodenitrification has been documented in laboratory experiments via reactions involving intermediates such as hydroxylamine (NH<sub>2</sub>OH) and NO<sub>2</sub><sup>-25</sup>. Hereafter, the term chemodenitrification refers to the abiotic reaction of Fe(II) and nitrite. The extent of N<sub>2</sub>O production via chemodenitrification versus denitrification is still poorly understood. Elevated levels of N<sub>2</sub>O have been observed in numerous studies examining iron- and nitrate-/nitrite-rich environments, e.g. soils<sup>26</sup>, hypersaline ponds and brines in Antarctica<sup>27</sup>, and marine coastal sediments<sup>28–30</sup>. However, these high levels of N<sub>2</sub>O have been solely attributed to microbial denitrification, potentially overlooking the important contribution of chemodenitrification to the overall N<sub>2</sub>O formation. Jones *et al.*<sup>31</sup> showed with a purely chemical laboratory setup that the co-presence of Fe<sup>2+</sup> and nitrite clearly stimulates chemodenitrification. They also provided an approach to distinguish between biotic versus abiotic contribution to N<sub>2</sub>O emission based on isotopic labelling. However, the actual role and potential of chemodenitrification in environmental systems remains unclear. The connection of the biogeochemical N and Fe cycle via chemodenitrification potentially impacts on the related microbial community. The production of Fe(III) minerals during chemodenitrification triggers heterotrophic Fe(III) reduction which supplies Fe<sup>2+</sup>, stimulating again chemodenitrification in the presence of nitrite, as well as microbial Fe(II) oxidation. Iron redox cycling is thus, strongly related to the biogeochemical N cycle. Based on microsensor measurements Wankel *et al.*<sup>30</sup> could show N<sub>2</sub>O formation at the interface of the nitrate and Fe(III) reduction zone within marine sediments. These authors hypothesized that chemodenitrification could play a major role in N<sub>2</sub>O production and hinted towards connections between the biogeochemical Fe and N cycle. Still, the actual contribution of chemodenitrification to N<sub>2</sub>O emission across the sediment-water interface remains unknown. Therefore, the focus of our study was to quantify the chemodenitrification-based N<sub>2</sub>O formation potential in natural marine sediments and to investigate the potential impact on the microbial community.

We hypothesize (i) that chemodenitrification plays an important role in marine sediments and that the abiotic oxidation of Fe(II) (provided by microbial Fe(III) reduction) by nitrite (formed during heterotrophic nitrate reduction) produces significant amounts of N<sub>2</sub>O, and (ii) that chemodenitrification may influence the N- and Fe-cycling microbial community in marine sediments.

Here we present incubation experiments with marine organic-rich sediment from the coastal area of the Baltic Sea, Norsminde Fjord, Denmark. Based on the knowledge gaps described above, the objectives of the present study were (i) to quantify N<sub>2</sub>O formation during chemodenitrification in microcosm studies, and (ii) to understand the consequences of chemodenitrifying conditions on the N- and Fe-cycling microbial community.

In our study, we found that up to 15–25% of total N<sub>2</sub>O production (range of three independent experiments) can be caused by chemodenitrification. This elevated N<sub>2</sub>O formation caused an increase of N<sub>2</sub>O reductase (*nosZ*) transcripts and an enrichment of potential Fe(II)-oxidizers and Fe(III)-reducers, as revealed by quantitative PCR and 16S rRNA (gene) amplicon sequencing, respectively. Our study demonstrates that chemodenitrification can contribute substantially to global N<sub>2</sub>O formation and significantly influences the N- and Fe-cycling microbial community in marine coastal sediments.

## Results

**Nitrite-induced (chemo)denitrification in coastal marine sediment.** The following experiments were set up: amendment of (i) nitrate and Fe(II) (Fig. 1), (ii) nitrite and Fe(II) (Fig. 1), (iii) nitrite only (Fig. S1) to both microbially active and sterilized sediments at concentrations to quantify the maximum contribution of chemodenitrification to N<sub>2</sub>O formation. In addition, one setup contained only native sediment (sterile vs. microbial active) (Fig. S1). The different setups are summarized in Table S1. In microcosms containing natural sediments, nitrite and Fe(II) were continuously produced and consumed via microbial and abiotic processes, and their resulting steady-state concentrations were low. In sterilized microcosms nitrite and Fe(II) were not produced during the experiment (Fig. S1). When N substrates and Fe(II) were added to the microbially active sediment, a maximum of 2653 ± 787.0 ppm of N<sub>2</sub>O (nitrate addition) and 4950 ± 748.6 ppm (nitrite addition) was quantified after four days of incubation (Fig. 1). This yielded a maximum amount of 5.8 ± 1.7 ppm (with nitrate) and 10.8 ± 1.6 ppm (with nitrite) per g wet sediment per hour for the respective microcosm setup. Thus, a maximum amount of N<sub>2</sub>O of 0.013 ± 0.001 μmol g<sup>-1</sup> h<sup>-1</sup> and 0.36 ± 0.1 μg N kg<sup>-1</sup> h<sup>-1</sup> (nitrate addition) and 0.024 ± 0.001 μmol g<sup>-1</sup> h<sup>-1</sup> and 0.68 ± 0.1 μg N kg<sup>-1</sup> h<sup>-1</sup> (nitrite addition) was formed (for calculations see Wang *et al.*<sup>26</sup>) (Fig. 2). The addition of Fe(II) and nitrate to sterilized sediment only showed a low production of 0.6 ± 0.03 ppm N<sub>2</sub>O per g wet sediment after four days of incubation, which relates to 1.3 ± 0.1 nmol g<sup>-1</sup> h<sup>-1</sup>. In contrast, the amendment of Fe(II) and nitrite to sterilized sediment revealed approximately three times more N<sub>2</sub>O production (1.9 ± 0.08 ppm N<sub>2</sub>O per g wet sediment per hour) which relates to 4.2 ± 0.1 nmol g<sup>-1</sup> h<sup>-1</sup>. Thus, a maximum of 17.4 ± 6.6% of total N<sub>2</sub>O (result of three independent microcosm experiments) was produced abiotically via chemodenitrification.

In nitrite-amended microcosms with microbially active sediment (without Fe(II) addition, Fig. S1), 1.87 ± 0.6 ppm N<sub>2</sub>O was formed per g wet sediment per hour, which relates to 4.2 ± 0.2 nmol N<sub>2</sub>O g<sup>-1</sup> h<sup>-1</sup>. For comparison, the sterile control setup that was amended with nitrite only produced 0.82 ± 0.4 ppm N<sub>2</sub>O per g wet sediment per hour, which relates to 2.4 ± 0.07 nmol g<sup>-1</sup> h<sup>-1</sup>. Almost no N<sub>2</sub>O was formed in native sterile and active microcosms within four days of incubation (<0.04 nmol N<sub>2</sub>O g<sup>-1</sup> h<sup>-1</sup>) (Fig. S1).

To evaluate the effect of iron and nitrogen substrates on the formation of N<sub>2</sub>O, we quantified the extractable and dissolved Fe(II), as well as total Fe, nitrate, nitrite, and dissolved organic matter (DOC) over time (Fig. 1). Extractable Fe(II) was relatively constant at approximately 31.7 ± 1.5 μmol wet g<sup>-1</sup> in the nitrate-/nitrite- and Fe(II)-amended (both microbially active and sterile setups) (Fig. 1). Whilst dissolved Fe(II) decreased in all

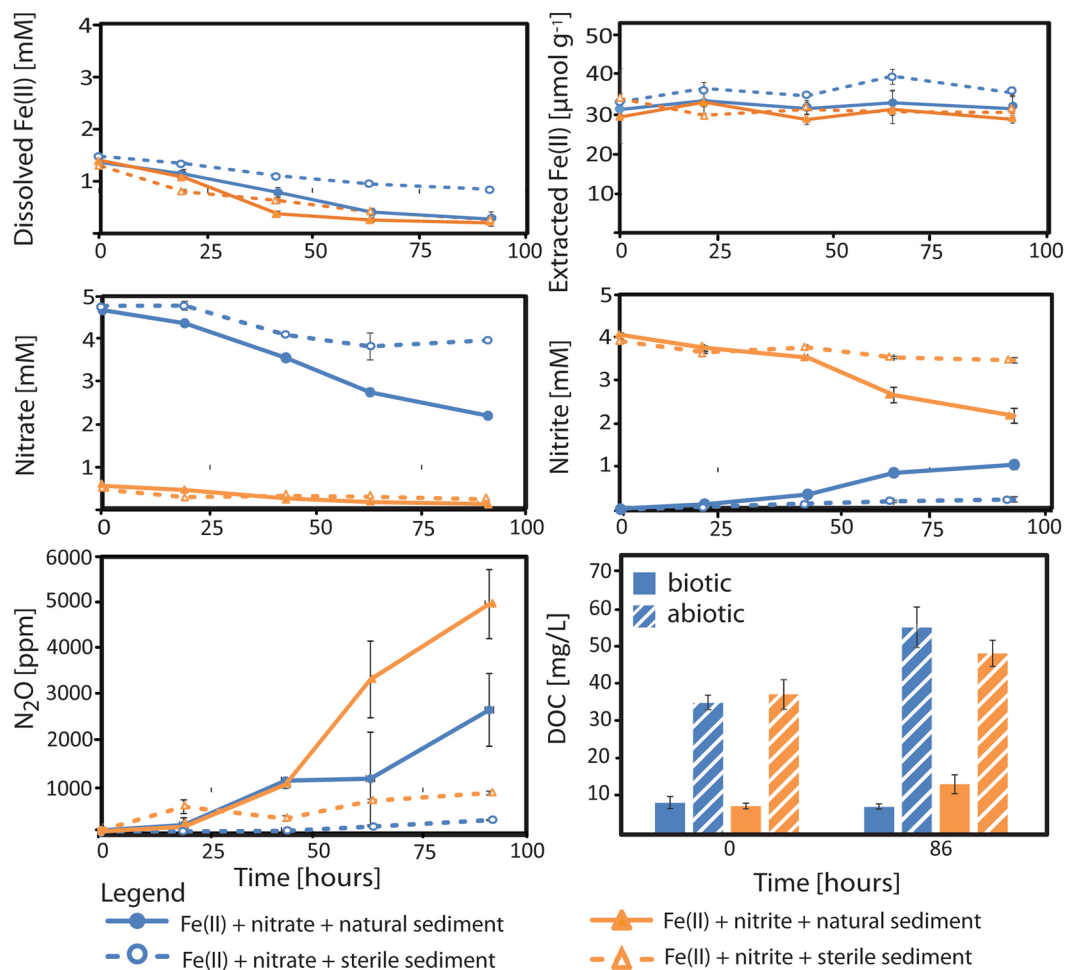


**Figure 1.** Sediment microcosms amended with dissolved Fe(II) and nitrate/nitrite. 4 mM nitrate and 2 mM FeCl<sub>2</sub> (shown in blue) or 4 mM nitrite and 2 mM FeCl<sub>2</sub> (shown in orange) were added to microbially active or sterilized marine Norsminde Fjord sediment collected in spring 2016 and N<sub>2</sub>O was quantified over time. Dissolved Fe(II) and nitrate/nitrite is shown in mM, extractable Fe(II) in μmol g<sup>-1</sup> wet sediment, N<sub>2</sub>O in ppm and DOC in mg/L. Results shown are average of three parallel microcosm setups (standard deviation is based on biological triplicates). Norsminde Fjord water without carbonate-buffer and additives had a DOC content of 4 mg/L.

setups containing both microbially active sediment and an amendment of nitrate or nitrite (from  $1.6 \pm 0.1$  mM to  $0.1 \pm 0.02$  mM and  $0.2 \pm 0.03$  mM, respectively), dissolved Fe(II) decreased from  $1.6 \pm 0.1$  to  $0.8 \pm 0.01$  mM in sterilized sediment with nitrate addition and from  $1.5 \pm 0.1$  to  $0.3 \pm 0.03$  mM in sterilized sediment with nitrite addition. The total extractable Fe(II) values and Fe<sub>total</sub> values were both approx.  $32.5 \pm 0.3$  μmol wet g<sup>-1</sup>. The nitrate concentration in microbially active sediment with nitrate addition decreased from  $4.7 \pm 0.02$  mM to  $2.2 \pm 0.1$  mM, probably due to nitrate reduction by denitrifying microorganisms (see Fig. S2; e.g. potential nitrate-reducers: *Sulfurimonas* and *Desulfuromonadales*). In the sterilized nitrate-amended sediments nitrate decreased to a much lower extent (from  $4.7 \pm 0.04$  mM to  $3.9 \pm 0.04$  mM). We observed a decrease of nitrite in nitrite-amended microbially active and sterilized setups (from  $4.0 \pm 0.04$  mM to  $2.7 \pm 0.2$  mM and to  $3.5 \pm 0.1$  mM, respectively) and an increase of nitrite in nitrate-amended microbially active and in sterilized setups (from 0 to  $0.9 \pm 0.1$  mM and  $0.2 \pm 0.01$  mM, respectively). Furthermore, the DOC content in sterilized sediment increased significantly, probably as a result from the gamma-radiation treatment. In contrast, in microbially active nitrite and Fe(II)-amended microcosms, the DOC increased only slightly while DOC even decreased in microbially active setups that were amended with nitrate and Fe(II) (probably due to denitrification activity) (Figs 1 and 2).

**Consequences of N<sub>2</sub>O formation and (chemo)denitrification for gene expression specific for the nitrogen cycle.** To evaluate the influence of (chemo)denitrification on active microbial nitrogen cycling, we followed gene and transcript copy numbers involved in the different denitrification steps (NO<sub>2</sub><sup>-</sup>, NO, and N<sub>2</sub>O reduction) during sediment incubation (Fig. 3). This was used to determine the effect of Fe(II)-, nitrate-, and nitrite-amendment on the microbial formation and reduction of N<sub>2</sub>O. Independent of the amendment, the copy

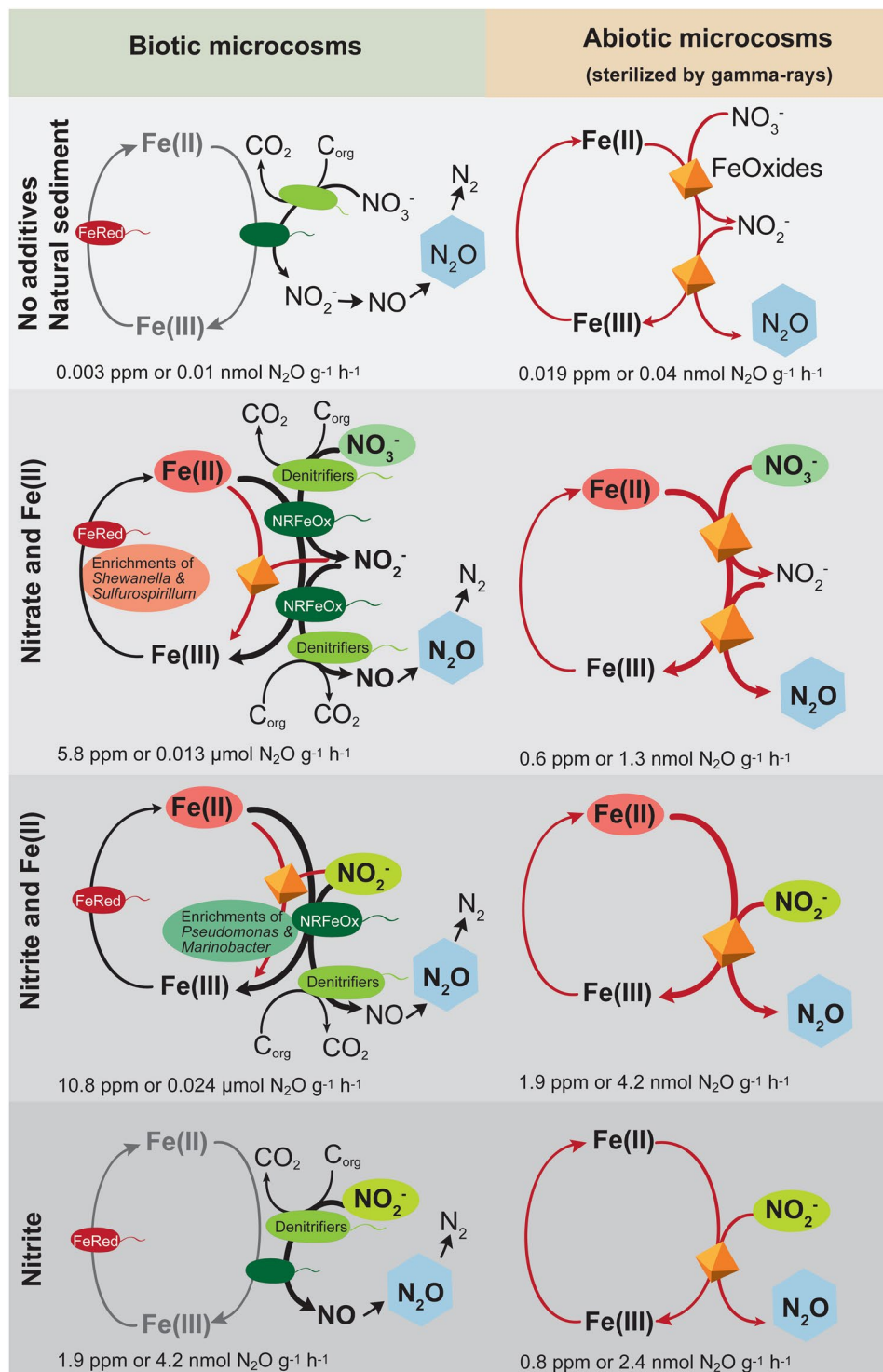


**Figure 2.** Conceptual model of the influences of nitrate or nitrite on microbial Fe-cycling and N<sub>2</sub>O production based on the detected N<sub>2</sub>O production rates [ppm g<sup>-1</sup> h<sup>-1</sup>] or [nmol g<sup>-1</sup> h<sup>-1</sup>]. The model is based on results of microcosm experiments with marine sediment from Norsminde Fjord amended with Fe(II) and nitrate, Fe(II) and nitrite (Fig. 1); or amended with nitrite only and native sediment (Fig. S1) (sterilized and microbially active setups). Thickness of lines and differences in symbol size indicate the relative importance. Heterotrophic denitrifiers are marked in light green, nitrate-reducing Fe(II)-oxidizers (NRFeOx) in dark green, and Fe(III)-reducers (FeRed) in red. Chemodenitrification reactions (abiotic reduction of nitrite by Fe(II), green rust or siderite) are highlighted in red. The orange mineral particle stands for iron minerals (e.g. FeOOH, green rust, siderite).

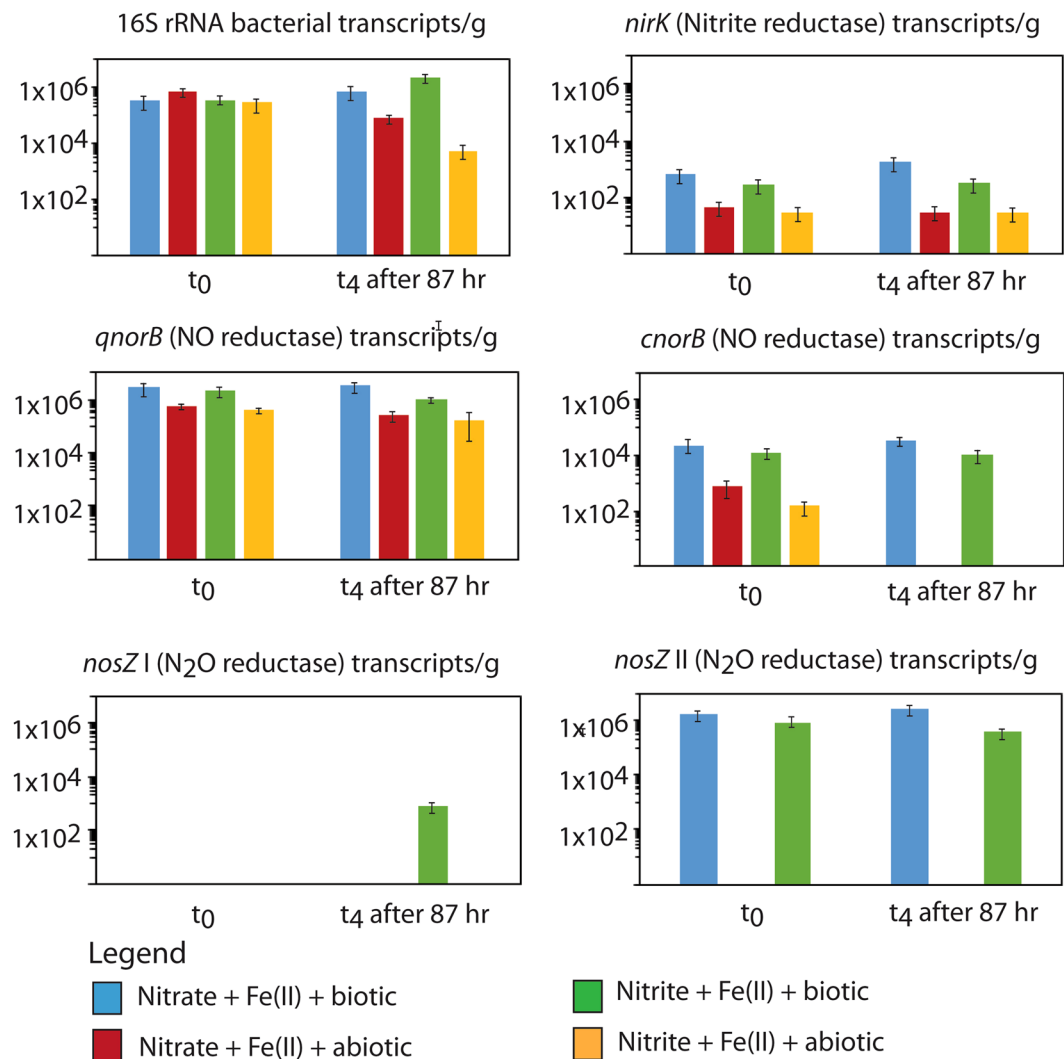


**Figure 3.** Absolute abundance of bacterial 16S rRNA and nitrogen cycle transcripts in biotic and abiotic microcosms (shown in Fig. 1). Transcripts in abiotic experiments were detectable. RNA might be stable due to inactivated RNase by gamma-rays<sup>41</sup>. Results based on DNA sequences are shown in Fig. S4. Results shown are average of three parallel microcosm setups. Standard deviation is based on biological triplicates (triplicate microcosm setups). g = gram wet weight. *nosZ I* = typical *nosZ*, clade I *nosZ*; *nosZ II* = atypical *nosZ*, clade II *nosZ*.

numbers for *nirK*, *qnorB*, *cnorB*, and atypical *nosZ* (clade II *nosZ*) did not change in the microbially active microcosms during incubation. Only, typical *nosZ* (clade I *nosZ*) was substantially upregulated in the active sediments that were amended with nitrite and Fe(II), whereas it was below the detection limit in all other samples (Fig. 3).

### Consequences of N<sub>2</sub>O formation by (chemo)denitrification on the Fe- and N-cycling microbial community.

In order to track the microorganisms that are involved in Fe- and N-cycling under denitrifying and chemodenitrifying conditions in our sediments, we analyzed the general microbial community in Fe(II)- and nitrate-/nitrite-amended microcosms (Fig. S2). We found that the addition of Fe(II), nitrate, and nitrite to the marine sediment and the resulting N<sub>2</sub>O formation caused a general microbial community shift based on DNA (present community) and RNA (active community) analysis (Fig. S2). The overall trends for the changes in the present and active microorganisms during microcosm incubation were similar, i.e. similar taxonomic groups were enriched in the DNA- and RNA-based analysis. Here, we present data for the RNA-based analyses. DNA-based results are provided in the supplementary information (Fig. S4).

The RNA-based 16S rRNA sequence analyses showed that the amendment of Fe(II) and nitrate followed by N<sub>2</sub>O formation through (chemo)denitrification led to the enrichment of active *Defluviicoccus* (*Rhodospirillales*) (1.3%), *Sulfurimonas* (*Campylobacterales*) (21.1%), and *Arcobacter* (*Campylobacterales*) (13.7%) (Fig. S2). *Defluviicoccus* sp. is a glycogen-accumulating organism and typically active in enhanced biological phosphorus removal-activated sludge systems<sup>32</sup>. While *Sulfurimonas* sp. are known for their ability of catalyzing chemolithotrophic reactions with ferrous iron and pyrite and the reduction of nitrate and nitrite<sup>33</sup>, *Arcobacter* sp. are known



for their activity in Fe-rich habitats<sup>34</sup>, their ability to catalyze Fe(III) and Mn(IV) reduction<sup>35</sup>, their use of Fe(III) citrate as electron acceptor<sup>36</sup>, and their nitrogen-fixation ability<sup>37</sup>.

In contrast, Fe(II) and nitrite amendment followed by N<sub>2</sub>O formation through (chemo)denitrification led to the enrichment of active *Psychrilyobacter* (*Fusobacteriales*) (6.3%), *Propionigenium* (*Fusobacteriales*) (2.2%), *Bacillus* (0.8%), *Thauera* (0.9%), and in particular *Marinobacter* (*Alteromonadales*) (22%) (Fig. S3). *Psychrilyobacter* is known as a psychrophilic Fe(III) reducer and was enriched in ferruginous marine sediments<sup>38</sup>. We identified abundant and active *Marinobacter* (22%) to be closely related to *M. litoralis* (100% 16S rRNA gene sequence similarity), to *M. aquaeolei* (99%; a potential neutrophilic Fe(II)-oxidizer), and to *M. hydrocarbonoclasticus* (99%). Relatives of *M. hydrocarbonoclasticus* were also identified recently based on *nosZ* gene sequence analysis in non-amended Norsminde Fjord sediment (Otte *et al.*, unpublished). *M. hydrocarbonoclasticus* has the genetic potential for all nitrogen cycle enzymes and the potential for N<sub>2</sub>O formation<sup>39</sup> while a close relative, i.e. *M. aquaeolei*, even has the potential for Fe(II) oxidation<sup>40</sup>.

**Evidence for the importance of chemodenitrification on N<sub>2</sub>O formation.** To distinguish between N<sub>2</sub>O formation by abiotic chemodenitrification and by microbially catalyzed processes, we inactivated the microbial community in the sediment by gamma-radiation. Gamma sterilization destroys enzymes (RNAses) that are required for RNA degradation<sup>41</sup>. However, even in sterilized samples traces of RNA were found (Fig. 3), which might result from incomplete sterilization. Still, the sterilized samples can be considered as a valid control setup. In order to evaluate the nitrate-reducing Fe(II)-oxidizing and the Fe(III)-reducing potential of the remaining RNA in the sterilized sediments, participation in nitrogen-converting metabolisms was checked using the *KEGG database* (*KEGG pathways*). Based on a previous strategic study on the efficiency of sterilization we can still consider gamma-radiation as the most efficient sterilization method for sediment samples<sup>41</sup>.

## Discussion

Our results show that chemodenitrification can account for up to 15–25% of the total N<sub>2</sub>O production in the marine sediments from Norsminde Fjord (Fig. 1). High N<sub>2</sub>O release in the presence of Fe(II) and nitrate/nitrite has been observed before in different environments<sup>27,30,42</sup>. For Norsminde Fjord previous studies reported N<sub>2</sub>O concentrations at the sediment-water/atmosphere interface of up to 0.49–4.9 μM<sup>43–45</sup>. Although, N<sub>2</sub>O emission rates are in a similarly high range compared to our data, the production of N<sub>2</sub>O has never been related to chemo-denitrification. The source of N<sub>2</sub>O formation has mainly been described to originate from heterotrophic denitrification or mixotrophic nitrate-dependent Fe(II) oxidation<sup>26</sup>. For the latter process, it has recently been shown that the oxidation of Fe(II) in the presence of nitrate and dissolved organic carbon, is a coupled abiotic-biotic reaction network (e.g. in *Acidovorax* sp. BoFeN1<sup>12</sup>). This means that nitrate gets microbially (heterotrophic) reduced and intermediate reactive nitrogen species (e.g. nitrite) are involved in chemodenitrification which produces N<sub>2</sub>O upon the oxidation of Fe(II)<sup>12</sup>. Few studies hypothesized that chemodenitrification might play a much bigger role in the N<sub>2</sub>O production patterns in ecological systems than previously thought<sup>25,30</sup>. Wankel *et al.*<sup>30</sup> showed that N<sub>2</sub>O increases in stratified marine coastal sediments as soon as oxygen is consumed along the redox gradient. These results in combination with our data imply the importance of N<sub>2</sub>O production due to chemodenitrification.

Anoxic conditions influence the expression of genes involved in the reduction of N oxides (Figs 3 and 4). Although the presence of elevated N<sub>2</sub>O concentrations was thought not to upregulate the expression of *nosZ* genes (within clade I of *nosZ*-harboring bacteria)<sup>46</sup>, recently, Harter *et al.*<sup>47</sup> suggested that the increase of typical *nosZ* expression under nitrate-reducing conditions might be due to locally enriched N<sub>2</sub>O. In our study, 46% more N<sub>2</sub>O was formed (after 91.5 hours of incubation) in microbially active microcosms that were amended with Fe(II) and nitrite (Fig. 1), compared to the microcosms that were amended with Fe(II) and nitrate only. In these microcosms elevated expression of typical *nosZ* was detected (Fig. 3). High N<sub>2</sub>O concentrations, as well as high nitrite levels, were described to have a toxic effect on the microorganisms, which might trigger the expression of typical *nosZ* genes as a detoxification mechanism<sup>48–51</sup>. The measured N<sub>2</sub>O and nitrite levels in our experiments only represent the net concentrations, and potentially the total N<sub>2</sub>O formed is underestimated. Based on thermodynamic considerations, the reduction of N<sub>2</sub>O to N<sub>2</sub> provides a higher energy yield than for the other denitrification steps<sup>48,52</sup>. Therefore, microorganisms that are capable of N<sub>2</sub>O reduction (e.g. *Shewanella* spp., *Marinobacter* spp., and *Pseudomonas* spp., which were enriched and active in our microcosms (Fig. S3)), might gain an energetic advantage over species performing the full denitrification pathway (with *nirK/S*, *nosZ*)<sup>53,54</sup>. This advantage is only available as long as anoxic and no sulfidic conditions are prevailing, as the presence of sulfide and oxygen can inhibit the expression of *nosZ* genes and the concurrent reduction of N<sub>2</sub>O to N<sub>2</sub>. Recently, a second clade of *nosZ* (atypical *nosZ*; clade II *nosZ*) was discovered and atypical *nosZ* were shown to be expressed in non-denitrifying N<sub>2</sub>O-reducing microorganisms<sup>49,54</sup>. Hallin *et al.*<sup>49</sup> proposed that clade II bacteria have a N<sub>2</sub>O respiratory chain that allows more efficient free energy conservation compared to the clade I system<sup>49</sup>. The energetic benefit from N<sub>2</sub>O reduction might explain the high expression of atypical *nosZ* in all setups. However, only bacteria with the full denitrification capacity are upregulating typical *nosZ* in the setup where high N<sub>2</sub>O concentrations (due to chemodenitrification) accumulate to cytotoxic levels<sup>47</sup>.

Our data show that nitrite-induced chemodenitrification has substantial consequences for the active N- and Fe-cycling microbial community (based on 16S rRNA gene sequences) (Figs 4 and S2, S3). Community members that carry the potential to trigger heterotrophic Fe(III) and nitrate reduction were enriched and active (Fig. S3), which is also supported by the slight decrease of DOC in nitrate and Fe(II) amended microcosms (Fig. 1). The stimulating effects of chemodenitrification on active Fe-cycling microorganisms (based on 16S rRNA gene sequences) were obvious by an increase of potential Fe(III)-reducers (*Arcobacter*, *Sulfospirillum*, and *Shewanella* in nitrate-amended setups, and *Psychrilyobacter* in nitrite-amended setups). In addition, an increase in the relative abundance of active Fe(II)-oxidizing bacteria [*Sulfurimonas* (with nitrate amendment), and *Marinobacter*

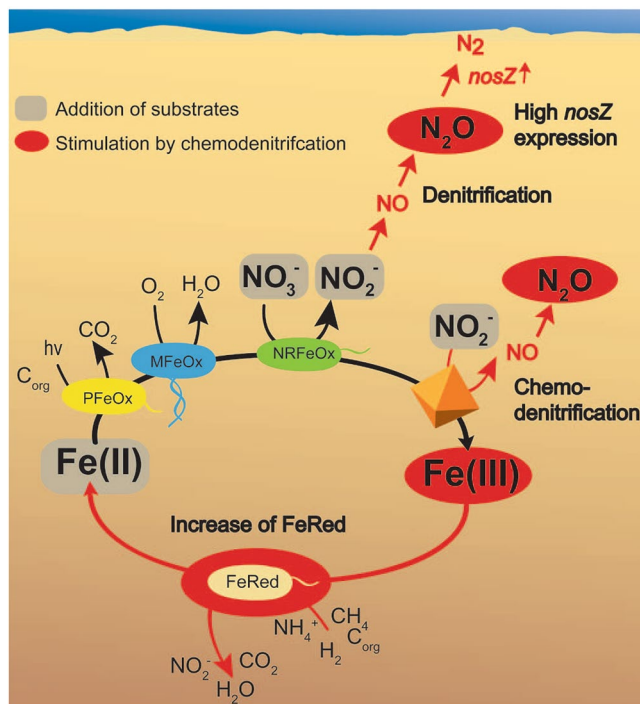


**Figure 4.** Cause and effects of nitrite- and nitrate-induced (chemo)denitrification-based  $\text{N}_2\text{O}$  formation in coastal marine sediment. When Fe(II) and nitrite/nitrate was added to the marine sediment, Fe(III) was formed among different process by chemodenitrification which is stimulating Fe(III)-reducing bacteria (FeRed). The FeRed bacteria then produce Fe(II) and stimulate Fe(II)-oxidizing bacteria. Therefore chemodenitrification has a significant impact on Fe-cycling in general. Simultaneously, nitrite/nitrate was reduced to NO and further to  $\text{N}_2\text{O}$  by chemodenitrification and denitrifying bacteria. In addition, the presence of high nitrite/nitrate concentration leads to a high typical *nosZ* gene expression in denitrifying bacteria which is responsible for the reduction of  $\text{N}_2\text{O}$  into  $\text{N}_2$ .

and *Pseudomonas* (with nitrite amendment)] has been confirmed by 16S rRNA gene sequence analysis (Fig. S3)). Several *Marinobacter* species have been found in Fe-rich habitats<sup>55</sup>, and their metabolic potential to utilize nitrate as terminal electron acceptors and iron (i.e.  $\text{FeS}_2$  and  $\text{CuFeS}_2$ ) as an electron donor has been demonstrated previously<sup>40,56</sup>. Potential Fe(III)-reducers (e.g. *Desulfobulbus*, *Desulfomusa*, *Sulfospirillum*, *Shewanella*) were more abundant and active than bacteria that might be enrolled in Fe(II) oxidation. These results are in line with previous studies that quantified significantly more Fe(III)-reducing bacteria (up to 2.8%) compared to Fe(II)-oxidizing bacteria (in particular nitrate-reducing Fe(II)-oxidizers with 0.3%) in the same sediment<sup>57,58</sup>. Potential denitrifying bacteria with typical *nosZ* such as *Shewanella* spp. (which are metabolically flexible, i.e. they can use either Fe(III), nitrate or nitrite, and were detected in nitrate-amended microcosms), *Pseudomonas* spp. and *Marinobacter* spp. (in nitrite-amended microcosms) were stimulated by nitrate/nitrite addition and chemodenitrification reactions (Fig. S3, selection of typical *nosZ* bacteria from Norsminde Fjord sediment).

The surviving community (*Xanthomonadales* clade JTB255, Candidatus *Isobeggiatoa divolgata*, *Oceanospirillales*, *Sandaracinaceae*, and *Bacteroidetes* at  $t_0$ ) and enriched microorganisms (e.g. *Synechococcus* and *Cyanobium* sp. at  $t_{\text{end}}$ ) in the gamma-sterilized microcosms (analyzed at both  $t_0$  and  $t_{\text{end}}$ ) (Fig. S2) have the ability of assimilatory nitrate reduction (reduction of nitrate to nitrite) but no genetic potential (e.g. no *nirK/S* and no *norB* genes) for further nitrite reduction. In addition, we did not see an increase of nitrite (Fig. 1) in microbially inactivated sediment. We can therefore conclude that all  $\text{N}_2\text{O}$  produced in gamma-radiated sediments can be attributed to an abiotic mechanism, namely chemodenitrification.

In this study we observed that up to 15–25% of total  $\text{N}_2\text{O}$  production might be caused by chemodenitrification, whereas 75–85% of  $\text{N}_2\text{O}$  was produced by denitrification and other microbial processes. 1.2 mM dissolved Fe(II) was consumed in microcosms with sterilized sediment, that were amended with 2 mM Fe(II) and 4 mM  $\text{NO}_2^-$  (Fig. 1). Following the stoichiometry of Equation 1, 1.2 mM Fe(II) can abiotically reduce 0.6 mM  $\text{NO}_2^-$ . The measured decrease in  $\text{NO}_2^-$  was approx. 0.5 mM  $\text{NO}_2^-$  (Fig. 1), and we can therefore consider chemodenitrification as the main process in the microcosm setup with sterilized marine sediment. In the microbially active setups 1.4 mM Fe(II) and 1.3 mM  $\text{NO}_2^-$  was consumed. Based on the stoichiometry of chemodenitrification the consumption of only 0.7 mM  $\text{NO}_2^-$  can be attributed to this process. The consumption of the remaining 0.7 mM  $\text{NO}_2^-$  can be related to various microbial processes in the sediment.

However, transferring our data to environmental systems we need to keep in mind several rate limiting factors for chemodenitrification. Compared to *in situ* conditions our setups do not suffer from substrate limitations, i.e.  $\text{Fe}^{2+}$  and nitrite production rates. Also, Fe-organic matter complexes, as they potentially occur in nature, will influence the reaction kinetics and the fate of Fe and N species<sup>59</sup>. In addition to that, in nature other processes,

| Geochemical parameters               |                                  |
|--------------------------------------|----------------------------------|
| Salinity                             | 14.6‰                            |
| pH anoxic porewater                  | 7.2                              |
| O <sub>2</sub> penetration depth     | 3.2 mm                           |
| Light penetration depth              | 2.2 mm                           |
| Fe(II) <sub>diss</sub> in sediment   | 73 ± 28 μmol g <sup>-1</sup> dw* |
| Fe(II) <sub>diss</sub> in porewater  | 29 ± 4.9 μM*                     |
| Fe(II) <sub>total</sub> in porewater | 106 ± 11 μM*                     |
| Nitrate (in porewater)               | 18.3 ± 8.2 μM*                   |
| Nitrite (in porewater)               | Below detection limit            |
| Sulfide (in porewater)               | Below detection limit            |
| DOC (in porewater)                   | 3.9 ± 0.1 mg l <sup>-1</sup> *   |
| TIC (in porewater)                   | 28.9 ± 0.1 mg l <sup>-1</sup> *  |

**Table 1.** Geochemical parameters of sediment from Norsminde Fjord in Denmark. Detailed sediment geochemistry description see Laufer *et al.*<sup>8</sup>. \*Mean value for measurements in the upper 3 cm of the sediments.

such as anammox, DNRA, and nitrate reduction by sulfur oxidation will impact the N<sub>2</sub>O emission rate<sup>60,61</sup>. Finally, the incubation temperature of 25 °C represents conditions that can be reached in summer months, especially when the overlying water column is very shallow<sup>62,63</sup>. Although these conditions do not represent average field site conditions over the whole year, they represent the environmental circumstances at which maximum N<sub>2</sub>O emission via chemodenitrification can be expected.

Coastal marine environments have been recognized as an important source of N<sub>2</sub>O to the atmosphere<sup>28,29</sup>. Sandy sediments, such as the one we used for our study, are representative for about 70% of all global shelf sediments<sup>64</sup> and are expected to release up to 1.9 Tg N<sub>2</sub>O-N yr<sup>-1</sup><sup>28</sup>. Assuming a contribution of 15–25% N<sub>2</sub>O release by chemodenitrification (data from this study) shelf sediments might account for 0.3–0.5 Tg N<sub>2</sub>O-N yr<sup>-1</sup> abiotically produced N<sub>2</sub>O. In the future the N<sub>2</sub>O release might even increase due to higher fertilizing activities in close-by agricultural fields. Leaching and runoff transport of nitrate into oceans leads to coastal marine eutrophication<sup>65</sup> and increases the potential for additional N<sub>2</sub>O production by (chemo)denitrification. There is a high chance that similarly high N<sub>2</sub>O emission rates that have been observed in many other environments, including soils<sup>26</sup> and sediments<sup>28–30</sup>, are triggered by chemodenitrification.

## Methods

**Site description and sampling procedure.** Marine sediment samples were taken in February 2015 April 2016, and March 2017 from the Aarhus Bay area (Denmark) (geochemical characterization is described in Laufer *et al.*<sup>58</sup> and Table 1). Sediment from the shallow marine estuary Norsminde Fjord (NS) was collected at 0.5 m water depth near its narrow entrance from Aarhus Bay (N 56°01.171'; E 010°15.390'). Bulk sediment from the upper 3 cm were collected, transported to the laboratory at 4 °C, and the sediment was stored for a few weeks at 4 °C until microcosm experiments were set up.

**Geochemical analyses.** Temperature, pH, salinity, and oxygen concentration of the water column were analyzed in the field with a multimeter (WTW, Multi 3430). The geochemical parameters of sediment water content, DOC, and nitrate concentrations in porewater as well as Fe(II) and Fe(III) concentrations in porewater and sediment were determined in the laboratory. All analyses are described in detail in Laufer *et al.*<sup>58</sup>.

**Microcosm experiment.** Bulk sediment from Norsminde Fjord was homogenized before setting up microcosm incubations. Microcosm incubations were set up in 100 ml serum vials that were wrapped in aluminum foil for dark incubations. Five g of homogenized bulk sediment and 50 ml anoxic filtered seawater were used for each microcosm. The headspace of the microcosms was N<sub>2</sub>/CO<sub>2</sub> (90:10). For preparation of the media, seawater was made anoxic by flushing with N<sub>2</sub> for at least 1 h per liter, filtering it through a 0.22 μm filter (EMD Millipore Steritop™) and replacing the headspace by N<sub>2</sub>/CO<sub>2</sub> (90:10), followed by adding 20 mM NaHCO<sub>3</sub> as buffer (final pH of the microcosms: 7.2 ± 0.1). To inhibit the activity of sulfate-reducing bacteria (and therefore inhibit reactions of sulfur species with Fe(II)) an anoxic and sterile filtered 1 M Na<sub>2</sub>MoO<sub>4</sub> solution was added to a final concentration of 20 mM<sup>58</sup>. The pH of the water was adjusted to 7.1 and regularly checked during incubation. The microcosms were amended with different substrates: (i) 2 mM Fe(II) (FeCl<sub>2</sub>) and 4 mM NO<sub>3</sub><sup>-</sup> (NaNO<sub>3</sub><sup>-</sup>), (ii) 2 mM Fe(II) (FeCl<sub>2</sub>) and 4 mM NO<sub>2</sub><sup>-</sup> (NaNO<sub>2</sub><sup>-</sup>), and (iii) 4 mM NO<sub>2</sub><sup>-</sup> only, each set of substrates added to native and sterilized sediment. The different setups are summarized in Table S1.

Abiotic control microcosms with gamma-sterilized sediment were incubated under the same conditions as the microbially active ones. Sediment for gamma-sterilization (sterile microcosm experiments) was filled into plastic bags, sent to Synergy Health Allershausen, Germany, and radiated at 52 kGy with 5% radiation tolerance. All microcosm experiments were setup in triplicates and incubated in dark at 25 °C. The chosen temperature represents conditions at which the observed processes will have a maximum environmental impact. Although the yearly average temperature in the field is significantly lower, the chosen temperature will be reached in summer months, especially when the water column is very shallow<sup>62,63</sup>.



**Quantification of Fe(II), nitrate, nitrite, and DOC.** For measuring Fe(II) and extractable Fe, 1 ml of slurry from each microcosm was sampled with a syringe inside an anoxic glovebox (100% N<sub>2</sub> atmosphere). 100 µl of this slurry sample was added to 900 µl 40 mM sulfamic acid in 1 M HCl and placed on a shaker (150 rpm) for 1 h (see Laufer *et al.*<sup>58</sup>). The samples were then centrifuged (5 min, 7000 g, Eppendorf 5430R) and the supernatant was used for Fe(II) and extractable Fe determination with the spectrophotometric Ferrozine assay<sup>21</sup>. The remaining part of the initial 1 ml sample of the slurry was centrifuged and the supernatant was used for analyses of the dissolved phase. The Fe-extraction with sulfamic acid<sup>21</sup> avoids the abiotic oxidation of Fe(II) by nitrite during acidic Fe-extraction. For nitrate and nitrite, 100 µl of supernatant was added to 900 µl Milli-Q H<sub>2</sub>O and stored anoxically at 4 °C until analysis by flow injection analysis (FIA)<sup>58</sup>. For analysis of DOC in microcosm incubations, 20 ml of sample was necessary<sup>58</sup> and the contents of sacrificial microcosms were centrifuged for 15 min at 5000 g (Hermle 7300 Germany). Afterwards, the supernatant was filtered through a 0.45 µm filter (MF-Millipore MCE membrane) and the DOC concentration was measured with a carbon analyzer (High TOC, Elementar, Germany).

**Nitrous oxide quantification.** For the determination of N<sub>2</sub>O concentrations, the pressure of the microcosm bottles was brought to normal pressure (1 bar) before sampling via a water trap. Headspace gas samples of 0.5 ml were taken from the microcosms 0, 15, 39, 63, and 87 hours after the beginning of the incubation and transferred into 22.5 ml evacuated gas chromatograph (GC) vials using a gas-tight syringe (1100TLL 100 ml Gastight, Hamilton, Reno, NV, USA). The trace gas concentrations in the GC vials (22.5 ml) were measured using a GC equipped with an electron capture detector (<sup>63</sup>Ni-ECD) for N<sub>2</sub>O and CO<sub>2</sub> (Hewlett Packard, 5890 Series II). The GC setup and configuration was described in detail previously<sup>66</sup>. Gas fluxes were calculated using the slope of the temporal change in concentration of the closed microcosms according to the equations published in Ruser *et al.*<sup>66</sup>. The result of 17% of total N<sub>2</sub>O by chemodenitrification is an average of three independent experiments and we show results of only one experiment.

**DNA and RNA extraction, DNA digestion, reverse transcription, and amplification.** Total DNA and RNA was extracted using the PowerSoil<sup>®</sup> RNA and DNA isolation kit as directed by the manufacturer (MO BIO Laboratories, Carlsbad, CA, USA), with the following modifications: 0.8 g to 2 g sediment was used from each sediment slice; 5 min bead-beating; centrifugation steps at maximal speed (7000 g) at 4 °C; and a longer incubation times at -20 °C (1.5–2.0 hours). RNA and DNA were eluted in 50 µl 10 mM Tris buffer. DNA and RNA concentrations were determined using a Qubit<sup>®</sup> 2.0 Fluorometer with DNA and RNA HS kits (Life Technologies, Carlsbad, CA, USA). RNA extracts were digested with the Ambion Turbo DNA-free<sup>™</sup> kit as directed by the manufacturer (Life technologies, Carlsbad, CA, USA). Successful DNA removal was confirmed by PCR using general bacterial primers (see Supplementary Information). Subsequent reverse transcription reactions were done using a reverse transcriptase (Invitrogen, Life Technologies) as described in the supporting information. Microbial 16S rRNA genes were amplified using primers 515F and 806R (see Supplementary Information) targeting the V4 region. Quality and quantity of the purified amplicons were determined using agarose gel electrophoresis and Nanodrop (NanoDrop 1000, Thermo Scientific, Waltham, MA, USA). Subsequent library preparation steps and sequencing were performed by Microsynth AG (Balgach, Switzerland). A sequence library was prepared and sequence adapters added using the Nextera kit. Sequencing was performed on an Illumina MiSeq sequencing system (Illumina, San Diego, CA, USA) using the 2 × 250 bp MiSeq Reagent Kit v2 (500 cycles kit) (Illumina, San Diego, CA, USA). The MiSeq reporter software v2.6 (Illumina, San Diego, CA, USA) was used for signal processing, de-multiplexing, and trimming of adapter sequences. The quality of the reads was checked with the software FastQC version 0.11.5 and the primers trimmed using cutadapt v1.14. Amplicon reads (accession number: SRP132652) have been deposited in the NCBI Genbank database (bioproject: PRJNA431287).

**Sequence analysis.** Demultiplexed and trimmed reads were further analyzed using QIIME (v1.9.1) (Caporaso reference). Paired end reads were joined using default settings and were further quality filtered and only those with a minimum Phred quality score of Q20 were used. Chimeric sequences were identified using usearch6.1<sup>67</sup> and removed. OTUs were picked using the QIIME workflow script “pick\_de\_novo\_otus.py” and taxonomically identified at 97% similarity using the SILVA 128 reference database<sup>68</sup>. Singletons were removed from the OTU table prior to further analysis. We used the quality-filtered reads for the graphs (Figs S2 and S3) and checked also with <0.1% filtered OTU tables (data not shown). Rarefaction curves, diversity indices (Shannon diversity, Simpson diversity), richness (Chao1, ACE), and coverage estimators (Good's coverage) were calculated using QIIME workflow scripts.

**Quantitative PCR of bacterial 16S rRNA genes and nitrogen cycle genes.** Quantification PCR (qPCR) specific for phylogenetic and functional marker genes [16S rRNA gene (Bacteria), *amoA* (Archaea), *nirK* (nitrite reductase), *qnorB* and *cnorB* (NO reductases), typical *nosZ* (clade I N<sub>2</sub>O reductase in denitrifiers) and atypical *nosZ* (clade II N<sub>2</sub>O reductase in non-denitrifiers)] was carried out using the SsoFast EvaGreen Supermix (Bio-Rad Laboratories, Hercules, CA, USA), an iQ5 real-time PCR detection system (iQ5 optical system software, version 2.0, Bio-Rad Laboratories), and gene-specific primers. For details on plasmid standards, gene-specific qPCR primers, reaction mixtures and thermal programs, please refer to Table S2 in the Supplementary Information.

## Data Availability

The microcosm datasets generated during and/or analyzed during the current study are available from the corresponding author on reasonable request.

## References

- Prather, M. J. *et al.* Measuring and modeling the lifetime of nitrous oxide including its variability. *J Geophys. Res. Atmos.* **120**, 5693–5705 (2015).
- Myhre, G. *et al.* Climate change 2013: the physical science basis. Contribution of working group I to the fifth assessment report of the intergovernmental panel on climate change. K., Tignor, M., Allen, S.K., Boschung, J., Nauels, A., Xia, Y., Bex, V. and Midgley, P.M., Cambridge University Press Cambridge, United Kingdom and New York, NY, USA (2013).
- Stein, L. Y. & Yung, Y. L. Production, isotopic composition, and atmospheric fate of biologically produced nitrous oxide. *Annu. Rev. Earth Planet. Sci.* **31**, 329–356, <https://doi.org/10.1146/annurev.earth.31.110502.080901> (2003).
- Crutzen, P. J. Photochemical reactions initiated by and influencing ozone in unpolluted tropospheric air. *Tellus* **26**, 47–57 (1974).
- Stocker, T. F. *et al.* (Ed.). IPCC. Climate change 2013: the physical science basis. Contribution of working group I to the fifth assessment report of the intergovernmental panel on climate change., 1535 (Cambridge University Press, 2013).
- Stein, L. Y. Surveying N<sub>2</sub>O-producing pathways in bacteria. *Method. Enzymol.* **486**, 131–152, [https://doi.org/10.1016/S0076-6879\(11\)86006-4](https://doi.org/10.1016/S0076-6879(11)86006-4) (2011).
- Ward, B. B., Arp, D. J. & Klotz, M. G. Nitrification PREFACE. *Nitrification*, Xiii–Xiv (2011).
- Zumft, W. G. Cell biology and molecular basis of denitrification. *Microbiol. Mol. Biol. Rev.* **61**, 533 (1997).
- Simon, J. & Klotz, M. G. Diversity and evolution of bioenergetic systems involved in microbial nitrogen compound transformations. *Biochim. Biophys. Acta* **1827**, 114–135, <https://doi.org/10.1016/j.bbabi.2012.07.005> (2013).
- Zhu, X., Burger, M., Doane, T. A. & Horwath, W. R. Ammonia oxidation pathways and nitrifier denitrification are significant sources of N<sub>2</sub>O and NO under low oxygen availability. *P Natl Acad Sci USA* **110**, 6328–6333, <https://doi.org/10.1073/pnas.1219993110> (2013).
- Wrage, N., Velthof, G. L., van Beusichem, M. L. & Oenema, O. Role of nitrifier denitrification in the production of nitrous oxide. *Soil Biol. Biochem.* **33**, 1723–1732, [https://doi.org/10.1016/S0038-0717\(01\)00096-7](https://doi.org/10.1016/S0038-0717(01)00096-7) (2001).
- Clueglein, N. *et al.* Potential Role of Nitrite for Abiotic Fe(II) Oxidation and Cell Encrustation during Nitrate Reduction by Denitrifying Bacteria. *Appl. Environ. Microb.* **80**, 1051–1061, <https://doi.org/10.1128/Aem.03277-13> (2014).
- Picardal, F. Abiotic and microbial interactions during anaerobic transformations of Fe(II). *Front. Microbiol.* **3**, 112, <https://doi.org/10.3389/fmicb.2012.00112> (2012).
- Campbell, M. A. *et al.* Model of the molecular basis for hydroxylamine oxidation and nitrous oxide production in methanotrophic bacteria. *FEMS Microbiol. Lett.* **322**, 82–89, <https://doi.org/10.1111/j.1574-6968.2011.02340.x> (2011).
- Liu, J. J., Wu, W. X., Ding, Y., Shi, D. Z. & Chen, Y. X. Ammonia-oxidizing archaea and their important roles in nitrogen biogeochemical cycling: a review. *Ying Yong Sheng Tai Xue Bao* **21**, 2154–2160 (2010).
- Kuenen, J. G. & Jetten, M. S. M. Extraordinary anaerobic ammonium-oxidizing bacteria. *Microbiol. Mol. Biol. Rev.* **67**, 456 (2001).
- Hu, H. W., Chen, D. & He, J. Z. Microbial regulation of terrestrial nitrous oxide formation: understanding the biological pathways for prediction of emission rates. *FEMS Microbiol. Rev.* **39**, 729–749 (2015).
- Torres, M. J. *et al.* Nitrous Oxide Metabolism in Nitrate-Reducing Bacteria: Physiology and Regulatory Mechanisms. *Adv. Microb. Physiol.* **68**, 353–432, <https://doi.org/10.1016/bs.ampbs.2016.02.007> (2016).
- Thomson, A. J., Giannopoulos, G., Pretty, J., Baggs, E. M. & Richardson, D. J. Biological sources and sinks of nitrous oxide and strategies to mitigate emissions. *Philos. Trans. R. Soc. Lond. B. Biol. Sci.* **367**, 1157–1168 (2012).
- Straub, K. L., Benz, M., Schink, B. & Widdel, F. Anaerobic, nitrate-dependent microbial oxidation of ferrous iron. *Appl. Environ. Microb.* **62**, 1458–1460 (1996).
- Bryce, C. *et al.* Microbial anaerobic Fe (II) oxidation—ecology, mechanisms and environmental implications. *Environ Microbiol* (2018).
- Clueglein, N. & Kappler, A. Abiotic oxidation of Fe (II) by reactive nitrogen species in cultures of the nitrate-reducing Fe (II) oxidizer *Acidovorax* sp. BoFeN1—questioning the existence of enzymatic Fe (II) oxidation. *Geobiology J.* **11**, 180–190 (2013).
- Melton, E. D., Swanner, E. D., Behrens, S., Schmidt, C. & Kappler, A. The interplay of microbially mediated and abiotic reactions in the biogeochemical Fe cycle. *Nat. Rev. Microbiol.* **12**, 797–808 (2014).
- Clark, F. E. Losses of nitrogen accompanying nitrification. *Trans. Int. Soc. Soil Sci.* 173–176 (1962).
- Zhu-Barker, X., Cavazos, A. R., Ostrom, N. E., Horwath, W. R. & Glass, J. B. The importance of abiotic reactions for nitrous oxide production. *Biogeochemistry* **126**, 251–267 (2015).
- Wang, M., Hu, R., Zhao, J., Kuzyakov, Y. & Liu, S. Iron oxidation affects nitrous oxide emissions via donating electrons to denitrification in paddy soils. *Geoderma* **271**, 173–180 (2016).
- Samarkın, V. A. *et al.* Abiotic nitrous oxide emission from the hypersaline Don Juan Pond in Antarctica. *Nat. Geosci.* **3**, 341 (2010).
- Seitzinger, S. P. & Kroeze, C. Global distribution of nitrous oxide production and N inputs in freshwater and coastal marine ecosystems. *Global Biogeochem. Cy.* **12**, 93–113 (1998).
- Bange, H. W. Nitrous oxide and methane in European coastal waters. *Estuar. Coast. Shelf Sci.* **70**, 361–374 (2006).
- Wankel, S. D. *et al.* Evidence for fungal and chemodenitrification based N<sub>2</sub>O flux from nitrogen impacted coastal sediments. *Nat. Comm.* **8**, 15595 (2017).
- Jones, L. C., Peters, B., Lezama Pacheco, J. S., Casciotti, K. L. & Fendorf, S. Stable isotopes and iron oxide mineral products as markers of chemodenitrification. *Environ. Sci. Technol.* **49**, 3444–3452 (2015).
- Burow, L. C., Kong, Y., Nielsen, J. L., Blackall, L. L. & Nielsen, P. H. Abundance and ecophysiology of *DeFluviicoccus* spp., glycogen-accumulating organisms in full-scale wastewater treatment processes. *Microbiology* **153**, 178–185 (2007).
- Kuenen, J. G. & Bos, P. Habitats and ecological niches of chemolitho(auto)trophic bacteria in *Autotrophic Bacteria* (ed. Schlegel, H. G. & Bowien, B.) 53–80 (Springer, 1989).
- Omeregıe, E. O. *et al.* Biogeochemistry and community composition of iron- and sulfur-precipitating microbial mats at the Chefred mud volcano (Nile Deep Sea Fan, Eastern Mediterranean). *Appl. Environ. Microbiol.* **74**, 3198–3215 (2008).
- Vandıeken, V. *et al.* Three manganese oxide-rich marine sediments harbor similar communities of acetate-oxidizing manganese-reducing bacteria. *ISME J.* **6**, 2078 (2012).
- Roalkvam, I. *et al.* Physiological and genomic characterization of *Arcobacter anaerophilus* IR-1 reveals new metabolic features in Epsilonproteobacteria. *Front. Microbiol* **6** (2015).
- Fera, M. T. *et al.* Detection of *Arcobacter* spp. in the coastal environment of the Mediterranean Sea. *Appl. Environ. Microbiol.* **70**, 1271–1276 (2004).
- Aromokeye, D. A. *et al.* Microbial interactions with crystalline iron oxides under varying temperature conditions. Goldschmidt Conference (Paris, France) (2017).
- Dell'Acqua, S., Pauleta, S. R., Moura, J. J. & Moura, I. Biochemical characterization of the purple form of *Marinobacter hydrocarbonoclasticus* nitrous oxide reductase. *Philos. Trans. R. Soc. Lond. B Biol. Sci.* **367**, 1204–1212 (2012).
- Singer, E. *et al.* Genomic potential of *Marinobacter aquaeolei*, a biogeochemical “opportunotroph”. *Appl. Environ. Microbiol.* **77**, 2763–2771 (2011).
- Otte, J. *et al.* Sterilization impacts on marine sediment – Are we able to inactivate microorganisms in environmental samples? *FEMS Microbiol. Ecol.* **94**, <https://doi.org/10.1093/femsec/fiy189> (2018).
- Pyzola, S. Nitrate reduction coupled to iron(II) and manganese(II) oxidation in an agricultural soil. Theses and Dissertations, University of Kentucky (2013).

43. Jørgensen, B. B. & Sørensen, J. Seasonal cycles of O<sub>2</sub> and reduction in estuarine sediments: the significance of an reduction maximum in spring. *Mar. Ecol. Prog. Ser.* **48**, 65–74 (1985).
44. Sørensen, J. Occurrence of nitric and nitrous oxides in a coastal marine sediment. *Appl. Environ. Microbiol.* **36**, 809–813 (1978).
45. Behrendt, A., De Beer, D. & Stief, P. Vertical activity distribution of dissimilatory nitrate reduction in coastal marine sediments. *Biogeosciences* **10**, 7509–7523 (2013).
46. Spiro, S. Nitrous oxide production and consumption: regulation of gene expression by gas-sensitive transcription factors. *Philos. Trans. R. Soc. Lond. B Biol. Sci.* **367**, 1213–1225 (2012).
47. Harter, J. *et al.* Gas entrapment and microbial N<sub>2</sub>O reduction reduce N<sub>2</sub>O emissions from a biochar-amended sandy clay loam soil. *Sci. Rep.* **6**, 39574 (2016).
48. Conthe, M., Kuenen, J. G., Kleerebezem, R. & van Loosdrecht, M. Exploring microbial N<sub>2</sub>O reduction: a continuous enrichment in nitrogen free medium. *Environ. Microbiol. Rep.* (2018).
49. Hallin, S., Philippot, L., Löffler, F. E., Sanford, R. A. & Jones, C. M. Genomics and ecology of novel N<sub>2</sub>O-reducing microorganisms. *Trends Microbiol.* <https://doi.org/10.1111/1758-2229.12615> (2017).
50. Poock, S. R., Leach, E. R., Moir, J. W., Cole, J. A. & Richardson, D. J. Respiratory detoxification of nitric oxide by the cytochrome nitrite reductase of *Escherichia coli*. *J. Biol. Chem.* **277**, 23664–23669 (2002).
51. Kern, M., Volz, J. & Simon, J. The oxidative and nitrosative stress defence network of *Wolinella succinogenes*: cytochrome c nitrite reductase mediates the stress response to nitrite, nitric oxide, hydroxylamine and hydrogen peroxide. *Environ. Microbiol.* **13**, 2478–2494 (2011).
52. Thauer, R. K., Jungermann, K. & Decker, K. Energy-conservation in chemotropic anaerobic bacteria. *Bacteriol. Rev.* **41**, 100–180 (1977).
53. Matocha, C., Dhakal, P. & Pyzola, S. The role of abiotic and coupled biotic/abiotic mineral controlled redox processes in nitrate reduction. *Adv. Agronomy* **115**, 181 (2012).
54. Jones, C. M., Graf, D. R., Bru, D., Philippot, L. & Hallin, S. The unaccounted yet abundant nitrous oxide-reducing microbial community: a potential nitrous oxide sink. *ISME J.* **7**, 417–426 (2013).
55. Handley, K. M. & Lloyd, J. R. Biogeochemical implications of the ubiquitous colonization of marine habitats and redox gradients by *Marinobacter* species. *Front. Microbiol.* **4** (2013).
56. Müller, M. *et al.* An Electrochemical Study of the Influence of *Marinobacter aquaeolei* on the alteration of hydrothermal chalcopyrite (CuFeS<sub>2</sub>) and pyrite (FeS<sub>2</sub>) under circumneutral conditions. *Geomicrobiol. J.* **31**, 373–382 (2014).
57. Otte, J. M. *et al.* The distribution of active iron-cycling bacteria in marine and freshwater sediments is decoupled from geochemical gradients. *Environ. Microbiol.* **20**, 2483–2499 (2018).
58. Laufer, K. *et al.* Anaerobic microbial Fe(II) oxidation and Fe(III) reduction in coastal marine sediments controlled by organic carbon content. *Environ. Microbiol.* **18**, 3159–3174 (2016).
59. Peng, C. *et al.* Oxidation of Fe (II)–Organic Matter Complexes in the Presence of the Mixotrophic Nitrate-Reducing Fe (II)-Oxidizing Bacterium *Acidovorax* sp. BoFeN1. *Environ. Sci. Technol.* **52**, 5753–5763 (2018).
60. Dalsgaard, T., Thamdrup, B. & Canfield, D. E. Anaerobic ammonium oxidation (anammox) in the marine environment. *Res. Microbiol.* **156**, 457–464 (2005).
61. Burgin, A. J. & Hamilton, S. K. Have we overemphasized the role of denitrification in aquatic ecosystems? A review of nitrate removal pathways. *Front. Ecol. Environ.* **5**(2), 89–96 (2007).
62. Dale, A. W. *et al.* Seasonal dynamics of the depth and rate of anaerobic oxidation of methane in Aarhus Bay (Denmark) sediments. *J. Mar. Res.* **66**, 127–155 (2008).
63. Jørgensen, K. S. & Sørensen, J. Two annual maxima of nitrate reduction and denitrification in estuarine sediment (Norsminde Fjord, Denmark). *Mar. Ecol. Prog. Ser.* **48**, 147–154 (1988).
64. Burdige, D. Estuarine and coastal sediments–coupled biogeochemical cycling. *Tr Estuar Coast. Sci.* **5**, 279–308 (2011).
65. Nixon, S. W. Coastal marine eutrophication: a definition, social causes, and future concerns. *Ophelia* **41**, 199–219 (1995).
66. Ruser, R., Schilling, R., Steindl, H., Flessa, H. & Beese, F. Soil compaction and fertilization effects on nitrous oxide and methane fluxes in potato fields. *Soil Sci. Soc. Am. J.* **62**, 1587–1595 (1998).
67. Edgar, R. C. Search and clustering orders of magnitude faster than BLAST. *Bioinformatics* **26**, 2460–2461 (2010).
68. Quast, C. *et al.* The SILVA ribosomal RNA gene database project: improved data processing and web-based tools. *Nucleic Acids Res.* **41**, D590–D596 (2012).

## Acknowledgements

We thank Katja Laufer (now at GEOMAR Kiel, Germany) for assistance in the field and helpful discussions. We additionally thank Ellen Struve for FIA measurements, Ulf Lüder for evaluation of geochemical data of the bulk sediments, and Akanksha Mishra for assistance in the lab. We are also grateful to Johannes Harter for helpful discussions and Daniel Straub for help with the sequencing data analysis. The authors acknowledge support by the High Performance and Cloud Computing Group at the Zentrum für Datenverarbeitung of the University of Tübingen. Funding was provided by the European Research Council under the European Union's Seventh Framework Program (FP/2007-2013)/ERC Grant, agreement no. 307320-MICROFOX and by ERC Advanced Grant (Grant No. 294200-MICROENERGY). S.K. is supported by an Emmy-Noether fellowship (grant # 326028733) from the German Research Foundation (Deutsche Forschungsgemeinschaft, DFG) through grant no INST 37/935-1 FUGG. C.S. is supported by a Margarete von Wrangell fellowship.

## Author Contributions

The study was jointly designed by J.O., C.S., S.K. and A.K. J.O. performed microcosm experiments, took gas samples and performed DNA and RNA extraction and further molecular biology work. R.R. quantified N<sub>2</sub>O and N.B. analyzed Illumina sequences. J.O., C.S. and A.K. wrote the manuscript, which was greatly improved by S.K. and N.B.

## Additional Information

**Supplementary information** accompanies this paper at <https://doi.org/10.1038/s41598-019-47172-x>.

**Competing Interests:** The authors declare no competing interests.

**Publisher's note:** Springer Nature remains neutral with regard to jurisdictional claims in published maps and institutional affiliations.



**Open Access** This article is licensed under a Creative Commons Attribution 4.0 International License, which permits use, sharing, adaptation, distribution and reproduction in any medium or format, as long as you give appropriate credit to the original author(s) and the source, provide a link to the Creative Commons license, and indicate if changes were made. The images or other third party material in this article are included in the article's Creative Commons license, unless indicated otherwise in a credit line to the material. If material is not included in the article's Creative Commons license and your intended use is not permitted by statutory regulation or exceeds the permitted use, you will need to obtain permission directly from the copyright holder. To view a copy of this license, visit <http://creativecommons.org/licenses/by/4.0/>.

© The Author(s) 2019